

Kinetics of endothelin-1 binding in the dog liver microcirculation in vivo

JOCELYN DUPUIS,¹ ANDREAS J. SCHWAB,² ANDRÉ SIMARD,² PETER CERNACEK,¹ DUNCAN J. STEWART,³ AND CARL A. GORESKY†^{2,4,5}

¹Department of Medicine, Montreal Heart Institute, Montreal H1T 1C8, ²McGill University Medical Clinic in the Montreal General Hospital, Departments of ⁴Medicine and

⁵Physiology, McGill University, Montreal, Quebec H3G 1A4, and ³Department of Medicine, St. Michael's Hospital, Toronto, Ontario, Canada M5B 1W8

Dupuis, Jocelyn, Andreas J. Schwab, André Simard, Peter Cernacek, Duncan J. Stewart, and Carl A. Goresky. Kinetics of endothelin-1 binding in the dog liver microcirculation in vivo. *Am. J. Physiol.* 277 (*Gastrointest. Liver Physiol.* 40): G905–G914, 1999.—Endothelin-1 (ET-1) is a 21-amino acid peptide produced by vascular endothelial cells that acts as a potent constrictor of hepatic sinusoids. Hepatic binding of tracer ¹²⁵I-labeled ET-1 was investigated in anesthetized dogs with the multiple-indicator dilution technique with simultaneous measurements of unlabeled immunoreactive ET-1 plasma levels. Despite 80% binding to albumin, tracer ¹²⁵I-ET-1 was avidly extracted by the liver, with only 15 ± 6% of the peptide surviving passage through the organ. Exchange of ET-1 between plasma and binding sites, probably located on the surface of liver cells, was quantitatively described by a barrier-limited, space-distributed variable transit time model. Reversible and irreversible parallel binding sites were found. Reversible and irreversible plasma clearances of unbound ¹²⁵I-ET-1 were 0.084 ± 0.033 ml·s⁻¹·g liver⁻¹ and 0.17 ± 0.09 ml·s⁻¹·g liver⁻¹, respectively, and the dissociation rate constant for reversible binding was 0.24 ± 0.12 s⁻¹. The specific ET_A receptor antagonist BMS-182874 did not modify binding to either site. The nonspecific ET_A/ET_B antagonist LU-224332 dose-dependently reduced irreversible binding only. ET-1 levels in the hepatic vein were significantly lower than in the portal vein but were not different from those in the hepatic artery. The ratio between hepatic vein and portal vein levels (0.64 ± 0.31) was considerably higher than survival fractions, suggesting a substantial simultaneous release of newly synthesized or stored ET-1 by the liver. These results demonstrate both substantial clearance and production of ET-1 by the intact liver. Hepatic ET-1 clearance is mediated by the ET_B receptor, with the presence of reversible, nonspecific ET-1 binding at the liver surface

endothelin clearance; endothelin receptor antagonist; protein binding; multiple indicator-dilution technique; vasoactive peptide; receptor-binding kinetics

ENDOTHELIN-1 (ET-1) is a 21-amino acid peptide produced by vascular endothelial cells and secreted preferentially in a paracrine fashion, with a smaller luminal secretion resulting in measurable plasma levels of this peptide. Its actions are mediated by two well-characterized receptor subtypes, ET_A and ET_B (7, 28). ET-1 is a

† Deceased 21 March 1996.

The costs of publication of this article were defrayed in part by the payment of page charges. The article must therefore be hereby marked "advertisement" in accordance with 18 U.S.C. Section 1734 solely to indicate this fact.

potent constrictor of the hepatic sinusoids (15), promotes glycogenolysis (31), and stimulates the release of humoral mediators by Kupffer cells (14). Hepatic stellate cells (also called Ito cells, fat-storing cells, or lipocytes), which are located in the Disse space where they act in a fashion similar to pericytes, are believed to be involved in hepatic vasoconstriction mediated by ET-1 (38). Hepatic stellate cells in culture contract in the presence of ET-1 in a dose-dependent way (24). Hepatocytes also possess high-affinity ET-1 binding sites that activate the phosphoinositide signal-transduction pathway (31). In contrast to cells from other organs, liver-derived cells respond to quite low levels of this peptide (14, 31).

Chronic liver disease is associated with increased serum ET-1 levels (26) and, in animal models, with an increase in hepatic ET-1 production (13). This may contribute to and/or reflect the disease process. The mixed ET_A and ET_B receptor antagonist bosentan has been shown to be effective in reducing carbon tetrachloride liver injury in rats, suggesting a contributing role of ET-1 in the pathological process (23). These findings connote the importance of endothelin for liver function and support a necessary entry of circulating ET-1 into the Disse space to interact with target cells.

In the rat, intravenously injected radioactive ET-1 has a very short plasma half-life of 7 min (1, 9, 32) and appears rapidly in tissues, predominantly in the lungs, followed in importance by the liver and the kidneys (1, 32). In the liver, it is deposited predominantly in hepatic stellate cells, followed by endothelial cells and to a lesser extent hepatocytes (10, 16). The autoradiographic lobular distribution of the immobilized ET-1 follows a gradient, with ET-1 levels diminishing from the portal to the centrolobular zone (16), a behavior typical for substances metabolized by the liver (19). In isolated rat liver cells, the binding of labeled ET-1 also occurs mainly in hepatic stellate cells, followed by the endothelial cells and hepatocytes (24). ET-1 is internalized and metabolized rapidly by hepatocytes in culture (11).

These observations suggest that the liver is an important site for the metabolism of circulating ET-1; on the other hand, the liver may be particularly sensitive to variations in the circulating levels of this peptide. To understand the dynamics of the hepatic action of ET-1, it is necessary to investigate its kinetic behavior, including the binding kinetics in a single pass through an organ. However, the above-mentioned studies were conducted in time frames of several minutes to

hours. Similarly, receptor-binding studies were ordinarily performed with incubation times of 10–60 min, with subsequent washing with buffers (10–12, 31, 35). These times are far longer than the transit time of plasma through an organ, which is on the order of seconds. To obtain an accurate picture of the dynamics of endothelin turnover in the mammalian body, the underlying events must be well understood, including their temporal behavior. In this study, we used the multiple-indicator dilution technique to assess reversible and irreversible binding of circulating ET-1 in livers of anesthetized dogs.

MATERIALS AND METHODS

The experiments were performed in anesthetized dogs with the multiple indicator-dilution technique. Three groups of animals were studied: in the first group ($n = 9$), no endothelin receptor antagonists were used; in the second group ($n = 11$), a nonspecific ET_A/ET_B receptor antagonist was administered; and in the third group ($n = 5$), a specific ET_A receptor antagonist was administered.

Animal preparation. Mongrel dogs were anesthetized with pentobarbital sodium (50 mg/kg iv), intubated, and allowed to spontaneously breathe room air. A median laparotomy was performed, and catheters were positioned in the portal vein (injection site) and in the hepatic vein (collection site) as previously described (17). To ensure adequate ventilation and hemodynamic stability, arterial blood pressure was continuously monitored through a right femoral arterial line, and arterial blood gases were obtained for analysis from the same line. A continuous electrocardiographic tracing was also recorded. For the nine experiments done in the absence of endothelin-receptor antagonists, 3-ml blood samples were taken from the portal vein, the hepatic vein, and the femoral artery for measurement of plasma immunoreactive ET-1 levels as previously described (5), and after completion of the experiment, the liver was surgically removed for determination of its wet weight.

Multiple-indicator dilution experiments. An injection mixture was prepared as previously described (4) that contained the various tracers to be studied. It was composed of the following three noneliminated tracers: ⁵¹Cr-labeled red blood cells (25 μ Ci), a marker of the vascular space; Evans blue-labeled albumin (5 mg Evans blue in 1 ml water), a marker of the plasma proteins of blood with limited diffusion into the Disse space; and [¹⁴C]sucrose (50 μ Ci), a tracer that diffuses into the Disse space. The fourth and only eliminated tracer in the preparation was ¹²⁵I-labeled ET-1 (5 μ Ci, specific activity 2,200 Ci/mM). Red blood cells were added to match the hematocrit of the dog. A minimal volume of 4-ml injection mixture was prepared; 2 ml were kept to serve as the portal vein injection bolus; the remainder was used to prepare three dose standards by adding 0.1 ml injection mixture to 0.9 ml of venous blood. Isotope crossover standards were prepared by adding small amounts of each indicator separately to venous blood.

This mixture (2 ml) was injected as a bolus through the portal vein catheter into the portal vein, and timed samples were simultaneously collected from a hepatic vein through the hepatic vein catheter, with a peristaltic pump and a rapid sample collector at 1-s intervals for a total of 40 s (17). To prevent clotting of the samples, each collection tube was preloaded with 5 ml heparin (10,000 IU/ml; Heparin Leo, Leo Laboratories, Ajax, ON). All tubes, including the dose and crossover standards, were then processed in the same fashion

to determine the activity of each tracer. The tubes were swirled for ~ 1 s (Vortex-Genie, Fisher Scientific, Ottawa, ON), an aliquot of 0.1 ml of blood was transferred to a new tube containing 1.5 ml of physiological saline, and 0.2 ml 1.5 M TCA was added to precipitate the proteins. The tubes were then inserted into a gamma counter (Cobra 5002, Canberra-Packard, Meriden, CT) for the determination of ⁵¹Cr and ¹²⁵I activity. After settling of the precipitate by gravity, 0.3 ml of supernatant was added to 5 ml aqueous liquid scintillation cocktail (Ready Safe, Beckman Instruments, Fullerton, CA) for determination of ¹⁴C activity in a liquid scintillation spectrometer (LS5801, Beckman). The remaining blood sample was centrifuged 10 min at 870 g , and 0.2 ml of the resulting plasma was added to 1 ml of physiological saline in a standard disposable spectrophotometer cuvette (1-cm path length; Fisher Scientific, Montreal, PQ) for determination of Evans blue absorbance at 620–740 nm in a spectrophotometer (HP 8452A, Hewlett Packard, Palo Alto, CA).

Effect of endothelin receptor antagonists on hepatic ET-1 kinetics. To gain more insight into the mechanisms responsible for hepatic ET-1 clearance, additional experiments were performed with intraportal injections of either the highly specific ET_A receptor antagonist BMS-182874 [constant of inhibition (K_i) for ET_A was 55 nM and for ET_B was 50 mM; Bristol-Myers Squibb, Princeton, NJ], or the mixed ET_A/ET_B receptor antagonist LU-224332 (K_i for ET_A was 3.5 nM and for ET_B was 7.2 nM; kindly provided by Michael Kirchengast, Knoll, Ludwigshafen, Germany). After completion of a first indicator-dilution experiment, the antagonists were directly injected into the portal vein followed by a second indicator-dilution experiment 5 min later. For each animal studied, only one injection of either BMS-182874 (50–800 mg) or LU-224332 (1–50 mg) was used.

Detection of ¹²⁵I-labeled metabolites in hepatic effluent. To determine whether ¹²⁵I-labeled ET-1 metabolites were present in the collected samples, we used the TCA precipitation method. With the use of this technique with HPLC control, Gandhi et al. (12) have shown that intact ¹²⁵I-ET-1 precipitates with albumin in the resulting pellet, whereas metabolites remain in the supernatant. Accordingly, to detect any metabolites of ¹²⁵I-ET-1, radioactivity was measured in 200- μ l aliquots of the supernatant resulting from TCA precipitation in all samples from five experiments.

Binding of ET-1 to plasma proteins. We added 0.2 μ Ci of ¹²⁵I-ET-1 (0.008 fM) to 300 ml of 4% PBS or dog plasma with increasing quantities of unlabeled ET-1, from 0.4 fM to 4.0 μ M (final concentrations of ET-1 from 0.04 pM to 12 μ M); this resulted in nine serial samples for each experimental condition. Ultrafiltration was performed as follows (30): the solutions were placed in the reservoirs of ultrafiltration units (Millipore Ultrafree-MC filter units, 10,000 NMWL) that had been pretreated with Sigmacoat (Sigma, St. Louis, MO) to prevent nonspecific ET-1 binding. The units were then centrifuged at 2,000 g for 20 min, resulting in an ultrafiltrate volume representing about 40% of the total. Aliquots of the unfiltered solutions and of the ultrafiltrates as well as the empty filter units were counted to determine the bound fraction of ET-1 as well as binding to the filter units. For all experiments combined, nonspecific binding to the filters was <1%.

Moment analysis of indicator dilution curves. The radioactivity determined in each outflow sample was divided by that determined in the samples from the injection mixture (corrected for the 1:10 sample dilution) and by the injection volume (22). Outflow profiles were thus presented as outflow tracer blood concentrations, normalized by dividing by the amount of tracer in the injection mixture, which corresponds

to fractional recoveries per milliliter of blood. Single-pass dilution curves were obtained by truncating the late portion of outflow profiles in which recirculation is apparent and applying exponential extrapolation (17). The areas under the curves were calculated by numerical integration (22). For noneliminated substances (red blood cells, albumin, and sucrose), this integral is equal to the inverse of blood flow (17). Recovery of ¹²⁵I-ET-1 was determined as the ratio between the area under the curve of its outflow profile and that of noneliminated substances (expected to be equal to each other). The mean transit time of each tracer through the system is then calculated as the time integral of the product of fractional recovery and time, divided by the time integrals of the fractional recoveries (22). The liver mean transit times were found by subtracting the transit time of the inflow and outflow catheters from those through the whole system.

Modeling of reference indicator kinetics. Outflow profiles for noneliminated indicators, such as red blood cells, sucrose, or albumin, can be described by the delayed-wave flow-limited model. In this model, the axial diffusional gradient is neglected, whereas exchange between the plasma, interstitial, and/or hepatocyte space is quasi-instantaneous (17). With the use of the red blood cells curve (C_{RBC}) as a reference, any diffusible tracer profile (C_{diff}) can be represented in this model with the following equation

$$C_{diff}(t) = \frac{1}{1 + \gamma_{diff}} C_{RBC} \left(\frac{t - t_0}{1 + \gamma_{diff}} + t_0 \right) \quad (1)$$

where γ_{diff} is the ratio between the extravascular and intravascular spaces accessed by the tracer and t_0 is a common large-vessel transit time (17). The equation implies that, after the large-vessel transit time, each point on the tracer outflow curve will be delayed in time relative to the corresponding point on the red blood cells curve by the factor $(1 + \gamma_{diff})$, and its magnitude will be decreased by the factor $1/(1 + \gamma_{diff})$. To take into account the distortion imposed by the input and collection catheters (21), the above relation (Eq. 1) was modified by deconvolution/convolution as previously developed (22). In the present experiments, the outflow catheter and the attached pump were the same as those characterized in this previous study.

Optimized parameters were obtained by a nonlinear least-squares procedure from Visual Numerics (Houston, TX) (22). The fit being performed simultaneously for all diffusible tracer profiles, the optimized parameters were t_0 and a space ratio, as defined above, for each tracer, for albumin (γ_{alb}) and for sucrose (γ_{suc}).

Modeling of ET-1 kinetics. Evaluation of the microcirculatory exchanges of ET-1 between liver cell and plasma was based on the barrier-limited space-distributed variable transit time model developed by Goresky et al. (19). The model describes the relationship between the outflow profile for the substance under study, $C_{ET-1}(t)$, and that of a reference substance, $C_{ref}(t)$, which is not taken up by the cells but behaves similarly in all other respects. Transfer of plasma ET-1 between the vascular and the Disse space was assumed to be extremely rapid (flow limited).

The original model includes three parameters describing influx and efflux across the liver cell membranes and intracellular sequestration or enzymic transformation. It has been proposed that this model is also applicable to the interaction between polypeptide hormones and cell surface receptors, as it occurs in receptor-mediated endocytosis (29). In this case, reversible association with and dissociation from cell surface receptors replaces influx and efflux, and sequestration from

the receptor to the cell interior replaces intracellular sequestration. This model will be referred to as the one receptor (or one binding site) model. However, for reasons discussed in RESULTS, we favor a model where removal of tracer ET-1 from plasma occurs by means of irreversible binding to specific receptors, and reversible binding to different binding sites without sequestration occurs in parallel (Fig. 1). This will be the parallel binding site model. It has been shown previously that sequestration from the plasma space and sequestration from the intracellular space yield identical outflow profiles with appropriate parameter transformation (18).

Previous experiments have suggested considerable reversible binding of endothelin to plasma albumin (34). Because of the limited access of plasma protein to the Disse space of the liver, such a binding could influence the outflow profile of ¹²⁵I-ET-1, and it needed to be addressed in this study. We therefore used a composite hypothetical reference indicator for which the apparent volume of distribution is related to those of sucrose (representing free plasma ¹²⁵I-ET-1) and albumin (representing ¹²⁵I-ET-1 bound to plasma proteins). Because of the very high single-pass ¹²⁵I-ET-1 extraction (86%), binding of ¹²⁵I-ET-1 to proteins was assumed to occur with very high association and dissociation rate constants (at least one order of magnitude faster than interaction with surface receptors) and thus no rate limiting effect on ¹²⁵I-ET-1 exchange between plasma and parenchymal cells. The appropriate reference curve for ¹²⁵I-ET-1 can then be calculated as a transformation similar to Eq. 1 applied to any diffusible tracer profile (here albumin was chosen) (37)

$$C_{ref}(t) = \frac{1 + \gamma_{alb}}{1 + \gamma_{ref}} C_{alb} \left(\frac{(t - t_0)(1 + \gamma_{alb})}{1 + \gamma_{ref}} + t_0 \right) \quad (2)$$

where γ_{ref} is the apparent space ratio between ¹²⁵I-ET-1 Disse space and sinusoidal plasma space, calculated as

$$\gamma_{ref} = (1 - f_u)\gamma_{alb} + f_u\gamma_{suc} \quad (3)$$

and f_u is ¹²⁵I-ET-1 unbound fraction.

By analogy to the original model by Goresky et al. (19) with appropriate parameter transformation (18), the outflow pro-

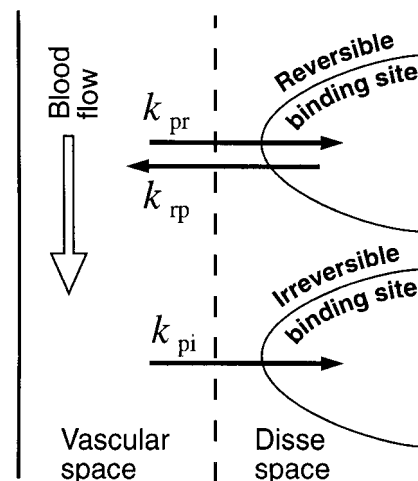


Fig. 1. Schematic representation of model of endothelin-1 (ET-1) receptor binding at level of a single sinusoid; k_{pr} , transfer coefficient for association to reversible binding site; k_{rp} , transfer coefficient for dissociation from reversible binding site; k_{pi} , transfer coefficient for association to irreversible binding site.

files for $^{125}\text{I-ET-1}$ in the parallel binding site model can be described by the following relation

$$C_{\text{ET-1}} = C_{\text{ref}}(t) e^{-(k_{\text{pi}} + k_{\text{pr}})(t - t_0)} + e^{-k_{\text{rp}}(t - t_0)} \int_{t_0}^t C_{\text{ref}}(\tau) e^{(k_{\text{rp}} - k_{\text{pi}} - k_{\text{pr}})(\tau - t_0)} \sum_{n=1}^{\infty} \frac{[k_{\text{pr}} k_{\text{rp}} (\tau - t_0)]^n [t - \tau]^{n-1}}{n!(n-1)!} d\tau \quad (4)$$

Because the fenestrated endothelial cells of the liver do not constitute a barrier to ET-1, the modeling of this process will be analogous to that of an enzymic process at the surface of the endothelial cells as considered by Goresky et al. (20) but with the use of an appropriate reference. The parameters describing the behavior of $^{125}\text{I-ET-1}$ tracer in this model are coefficients of tracer transfer between a mobile (plasma) compartment (p), represented by the combination of the vascular and Disse plasma spaces, and a stationary compartment (r), representing reversible binding sites on the surface of parenchymal cells. The transfer coefficient for rapid receptor binding or association is k_{pr} , that for dissociation from receptors is k_{rp} , that for irreversible sequestration is k_{pi} , all with units of a reciprocal time (s^{-1}). Again, Eq. 4 was modified by deconvolution/convolution (22). The parameters were optimized with a least-square algorithm.

The unidirectional plasma clearances per gram liver for $^{125}\text{I-ET-1}$ for reversible binding (CL_{pr}) and irreversible sequestration (CL_{pi}) were computed as the products of influx transfer coefficient and the sum of sinusoidal plasma and Disse spaces as shown below

$$\text{CL}_{\text{pr}} = f_{\text{u}} k_{\text{pr}} (1 - \text{Hct}) F (\bar{t}_{\text{suc}} - t_0) \quad (5)$$

$$\text{CL}_{\text{pi}} = f_{\text{u}} k_{\text{pi}} (1 - \text{Hct}) F (\bar{t}_{\text{suc}} - t_0) \quad (6)$$

where Hct is hematocrit, F is liver blood flow, and \bar{t}_{suc} is sucrose mean transit time.

RESULTS

Binding of ET-1 to plasma proteins. The ultrafiltration experiments revealed considerable and similar binding of $^{125}\text{I-ET-1}$ to BSA and dog plasma proteins. The unbound fraction was similar for all concentrations of ET-1 (from 0.04 pmol/l to 12 $\mu\text{mol/l}$), with a mean of $f_{\text{u}} = 0.20 \pm 0.04$ for BSA and $f_{\text{u}} = 0.22 \pm 0.05$ for dog plasma.

Outflow profile of noneliminated indicators. Representative sets of dilution curves obtained after injection of the tracers into the portal vein and collection from a hepatic vein are shown in Fig. 2. The typical behavior of the noneliminated tracers, red blood cells, albumin, and sucrose has been extensively described previously (17). According to the delayed wave flow limited model, each tracer is delayed and diluted compared with the intravascular reference, red blood cells, by virtue of its own larger volume of distribution in the liver. The results of the analysis of the noneliminated indicators are assembled in Table 1. The recoveries for the noneliminated tracers were essentially complete within experimental error (their areas under the curves being equal). The parameters obtained from the simultaneous fit of red blood cells, albumin, and sucrose experimental profiles are compiled in Table 2.

Effect of the endothelin receptor antagonists on the recovery and outflow profile of $^{125}\text{I-ET-1}$. In the absence of endothelin receptor antagonists, apart from its much smaller fractional recovery, tracer $^{125}\text{I-ET-1}$ exhibits an outflow profile closely related to that of tracer albumin. This is consistent with the finding of 80% binding of ET-1 to serum albumin and supports the use of albumin as a reference indicator for the description of tracer $^{125}\text{I-ET-1}$ kinetics in the liver. The mean single-pass hepatic fractional recovery of $^{125}\text{I-ET-1}$ in the absence of antagonists was quite small (Table 3), with an overall

Fig. 2. Representative sets of outflow dilution curves from control conditions (A and B) and after either nonspecific ET-receptor antagonist (C) or specific ET_A receptor antagonist (D). Data are truncated before recirculation occurs, and extrapolation (dashed lines) was according to terminal slopes on this logarithmic representation.

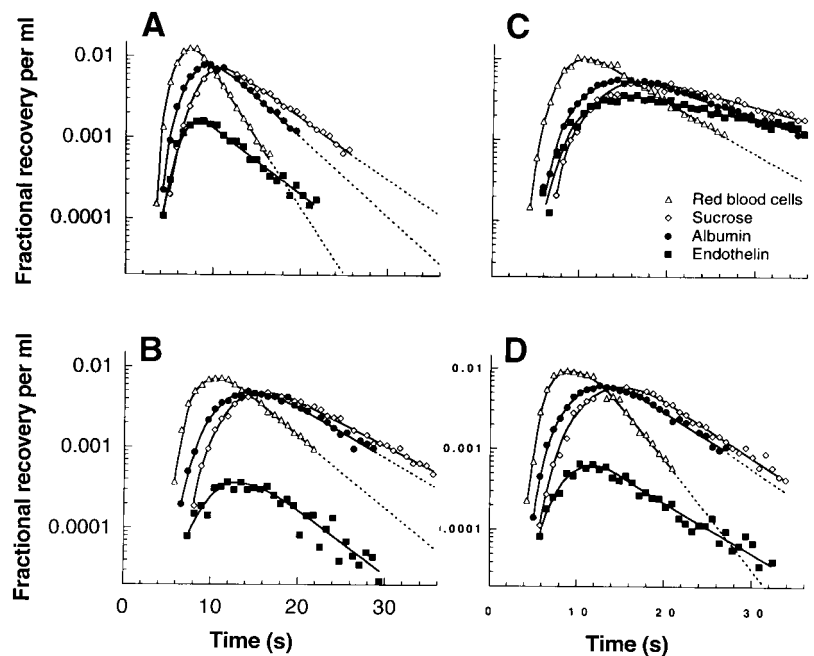


Table 1. Parameters obtained from the analysis of experimental profiles

	<i>n</i>	Dog Weight, kg	Blood Flow, ml/s	\bar{t}_{RBC} , s	\bar{t}_{alb} , s	\bar{t}_{suc} , s
Experiments without antagonist	9	21 ± 5	11.5 ± 5.7	11.5 ± 2.5	15.3 ± 4.3	19.8 ± 6.0
Nonspecific antagonist experiments						
Control	11	22 ± 4	11.8 ± 4.3	10.5 ± 4.0	15.2 ± 4.8	17.2 ± 5.6
Antagonist			10.2 ± 3.8	11.4 ± 3.7	17.5 ± 5.3	20.1 ± 6.2
ET _A antagonist experiments						
Control	5	24 ± 2	11.5 ± 4.5	11.1 ± 2.4	16.5 ± 3.3	18.5 ± 3.5
Antagonist			10.3 ± 3.1	10.1 ± 1.6	15.0 ± 2.3*	17.2 ± 2.7

Values are means ± SD. \bar{t}_{RBC} , \bar{t}_{alb} , and \bar{t}_{suc} , Mean transit times for red blood cells, albumin, and sucrose, respectively. * *P* < 0.5, antagonist vs. controls.

mean of 0.15 ± 0.06 for the 25 experiments performed in the absence of antagonists. The specific ET_A receptor antagonist BMS-182874 did not modify tracer ¹²⁵I-ET-1 outflow profiles and recoveries, even at the very high dose of 400 mg (Fig. 2 and Table 3). On the other hand, the mixed ET_A/ET_B receptor antagonist LU-224332 caused an upward shift in the ¹²⁵I-ET-1 outflow profile and an increase in ¹²⁵I-ET-1 recovery, which depended on the dose and attained a range between 0.76 and 0.80 at the highest dose of 50 mg. The analysis of ¹²⁵I-ET-1 outflow profile after administration of the mixed antagonist then becomes critical in the choice of a model that will best describe hepatic kinetics of this peptide. The upslope portion of the ¹²⁵I-ET-1 curve, from appearance to peak (Fig. 2, top right), is below that of albumin, with mild progressive separation of the curves attributed to the mild hepatic removal of ¹²⁵I-ET-1. The downslope portion of the ¹²⁵I-ET-1 curve, however, progressively approaches that of albumin and, later in time, crosses over. This pattern is typical of substances that exhibit reversible hepatic binding. The late returning component represents a progressively decreasing instantaneous extraction compared with the vascular reference. We found no detectable ¹²⁵I-ET-1 metabolites in the supernatants of TCA precipitation of the hepatic effluent, suggesting that this small returning component represents intact ¹²⁵I-ET-1.

Endothelin binding in the liver: ET-1 is known to bind to its receptors with high affinity and a slow dissociation rate. Accordingly, one would not expect any returning component, and if a reversible binding site did exist,

the returning component should be proportionally reduced after receptor blockade. This is not supported by the present data; despite substantial reduction in hepatic ¹²⁵I-ET-1 removal after injection of the mixed antagonist, the returning component of ¹²⁵I-ET-1 persisted and even became more prominent on the outflow profile as ¹²⁵I-ET-1 recovery increased. The one reversible binding site model was therefore rejected and a two binding site model was adopted (Fig. 1). This model describes a irreversible binding site in parallel with a reversible binding site without sequestration.

The optimal parameters obtained from the fits of this model are compiled in Table 3. The variation of the clearances with liver blood flow for the nine experiments performed without endothelin-receptor antagonists is shown in Fig. 3. The Pearson correlation coefficients obtained by performing error-weighted regression between the clearances and liver blood flow are 0.90 and 0.99 for CL_{pr} and CL_{pi}, respectively. This behavior, previously described for rubidium uptake (22), is tentatively attributed to flow recruitment of sinusoids.

The effects of the antagonists on hepatic ¹²⁵I-ET-1 extraction and the model-derived transfer coefficients are more easily appreciated when the ratios of these parameters, measured before and after injection of the antagonists, are plotted as a function of the increasing antagonist doses (Fig. 4). Hepatic ¹²⁵I-ET-1 extraction was dose-dependently decreased by the mixed ET_A/ET_B antagonist but remained unaffected by comparatively large doses of the specific ET_A antagonist. The transfer

Table 2. Parameters obtained from the simultaneous fit of red blood cells, albumin and sucrose experimental profiles

	<i>n</i>	<i>t</i> ₀ , s			γ _{alb}			γ _{suc}		
		Mean	±SD _I	±SD _U	Mean	±SD _I	±SD _U	Mean	±SD _I	±SD _U
Experiments without antagonist	9	2.6	0.8	0.4	0.48	0.21	0.04	1.15	0.48	0.05
Nonspecific antagonist experiments										
Control	11	2.5	1.1	0.4	0.67	0.14	0.07	1.05	0.24	0.07
Antagonist		2.6	1.3	0.3	0.77	0.18	0.05	1.24	0.37	0.06
ET _A antagonist experiments										
Control	5	2.5	1.2	0.4	0.67	0.20	0.05	1.01	0.35	0.06
Antagonist		2.7	0.9	0.3	0.72	0.04	0.05	1.10	0.13	0.06

Values are means ± SD. *t*₀, Large-vessel transit time; γ_{alb} and γ_{suc}, ratios between accessed Disse space and sinusoidal space for albumin and sucrose; SD_I, interindividual standard deviation; SD_U, average standard deviation calculated for each experiment using the matrix of sensitivities from the fit, representing uncertainty on optimized parameter.

Table 3. Parameters obtained from the fit of endothelin profiles

Exp. No.	Antagonist Dose, mg	ET-1 Recovery		k_{pr} , s ⁻¹		k_{rp} , s ⁻¹		k_{pi} , s ⁻¹	
		Control	Antagonist	Control	Antagonist	Control	Antagonist	Control	Antagonist
Experiments without antagonist									
1		0.13		0.108 ± 0.023		0.30 ± 0.15		0.296 ± 0.015	
2		0.11		0.114 ± 0.024		0.46 ± 0.13		0.314 ± 0.008	
3		0.27		0.103 ± 0.145		0.11 ± 0.15		0.193 ± 0.164	
4		0.15		0.075 ± 0.011		0.16 ± 0.06		0.186 ± 0.010	
5		0.11		0.127 ± 0.015		0.24 ± 0.04		0.220 ± 0.005	
6		0.17		0.072 ± 0.013		0.11 ± 0.07		0.178 ± 0.019	
7		0.08		0.088 ± 0.017		0.24 ± 0.08		0.176 ± 0.006	
8		0.19		0.126 ± 0.008		0.16 ± 0.03		0.227 ± 0.007	
9		0.15		0.153 ± 0.021		0.35 ± 0.06		0.153 ± 0.004	
Nonspecific antagonist experiments									
1	1	0.12	0.18	0.039 ± 0.014	0.044 ± 0.008	0.29 ± 0.12	0.12 ± 0.05	0.164 ± 0.006	0.150 ± 0.007
2	5	0.10	0.27	0.223 ± 0.036	0.144 ± 0.014	0.52 ± 0.09	0.26 ± 0.06	0.312 ± 0.006	0.150 ± 0.008
3	5	0.08	0.17	0.104 ± 0.026	0.069 ± 0.007	0.31 ± 0.11	0.21 ± 0.04	0.125 ± 0.005	0.089 ± 0.002
4	10	0.13	0.50	0.233 ± 0.052	0.102 ± 0.018	0.66 ± 0.17	0.14 ± 0.09	0.273 ± 0.008	0.062 ± 0.025
5	10	0.11	0.48	0.419 ± 0.095	0.330 ± 0.072	0.72 ± 0.19	0.48 ± 0.15	0.340 ± 0.013	0.133 ± 0.011
6	20	0.26	0.60	0.118 ± 0.027	0.064 ± 0.010	0.48 ± 0.11	0.14 ± 0.08	0.122 ± 0.003	0.040 ± 0.011
7	20	0.09	0.59	0.135 ± 0.022	0.111 ± 0.008	0.34 ± 0.06	0.18 ± 0.03	0.220 ± 0.005	0.037 ± 0.003
8	20	0.08	0.62	0.364 ± 0.058	0.149 ± 0.008	0.78 ± 0.13	0.20 ± 0.02	0.371 ± 0.008	0.040 ± 0.002
9	50	0.17	0.80	0.111 ± 0.026	0.152 ± 0.016	0.43 ± 0.14	0.38 ± 0.05	0.225 ± 0.008	0.020 ± 0.001
10	50	0.19	0.79	0.102 ± 0.011	0.060 ± 0.007	0.31 ± 0.05	0.17 ± 0.04	0.218 ± 0.004	0.013 ± 0.002
11	50	0.09	0.76	0.131 ± 0.017	0.108 ± 0.005	0.34 ± 0.06	0.16 ± 0.01	0.260 ± 0.005	0.026 ± 0.002
ET _A antagonist experiments									
1	50	0.08	0.09	0.119 ± 0.027	0.178 ± 0.042	0.45 ± 0.12	0.56 ± 0.15	0.283 ± 0.008	0.301 ± 0.009
2	100	0.07	0.09	0.243 ± 0.034	0.133 ± 0.013	0.43 ± 0.07	0.38 ± 0.06	0.341 ± 0.007	0.271 ± 0.004
3	200	0.08	0.11	0.123 ± 0.021	0.126 ± 0.020	0.46 ± 0.10	0.35 ± 0.07	0.200 ± 0.004	0.200 ± 0.005
4	300	0.07	0.08	0.254 ± 0.053	0.438 ± 0.082	0.79 ± 0.16	0.79 ± 0.15	0.236 ± 0.004	0.313 ± 0.008
5	400	0.06	0.09	0.162 ± 0.037	0.280 ± 0.047	0.57 ± 0.15	0.59 ± 0.10	0.225 ± 0.006	0.244 ± 0.005

Values are means ± SD estimated using the matrix of sensitivities from the fit, representing uncertainty on optimized parameter. k_{pr} and k_{rp} , Transfer coefficients for association to and dissociation from reversible hepatic binding sites respectively; k_{pi} , transfer coefficient for association to irreversible hepatic binding sites.

coefficient for binding of ¹²⁵I-ET-1 to the irreversible site (k_{pi}) behaved similarly, exhibiting a marked dose-dependent reduction only with the mixed ET-1 receptor antagonist. The fitted coefficients for association to (k_{pr}) and dissociation from (k_{rp}) the reversible binding site show considerable scatter around the line of unity, with large standard errors (Fig. 4). No dose-dependent effect is evident for either antagonist. For the specific ET_A

antagonist, the ratios for k_{pr} tend to be higher than the line of unity, and for the experiments performed with the mixed antagonist, the ratios for both k_{pr} and k_{rp} tend to be lower than the line of unity.

With the use of the model-derived parameters, the experimental hepatic outflow profile for ¹²⁵I-ET-1 can be divided into its throughput and returning components (Fig. 5). The former represents ¹²⁵I-ET-1 that has transited through the liver without any interaction with binding sites, whereas the latter is composed of ¹²⁵I-ET-1 returning to circulation after reversible binding. After administration of the nonspecific antagonist, both throughput and returning components were increased.

Immunoreactive ET-1 levels. The mean values for ET-1 levels were 0.46 ± 0.35 pmol/l in the portal vein, 0.36 ± 0.36 pmol/l in the hepatic vein, and 0.35 ± 0.37 pmol/l in the hepatic artery (Fig. 6). The average ratio to portal vein ET-1 levels was 0.64 ± 0.33 for hepatic vein levels and 0.59 ± 0.31 for hepatic artery levels. ET-1 levels in the hepatic vein or the hepatic artery were significantly lower than the ones in the portal vein (paired *t*-test; probability that levels are the same is *P* < 0.01 in both cases), whereas no significant difference was found between hepatic artery and hepatic vein. One subject had markedly elevated levels of over 1

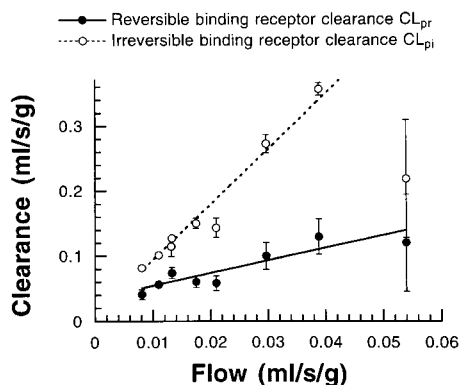


Fig. 3. Variation of influx reversible binding (CL_{pr}) and irreversible binding (CL_{pi}) clearances per gram liver with flow. Dashed line is linear regression of data. Error bars represent standard deviations as measures of reliability from fit.

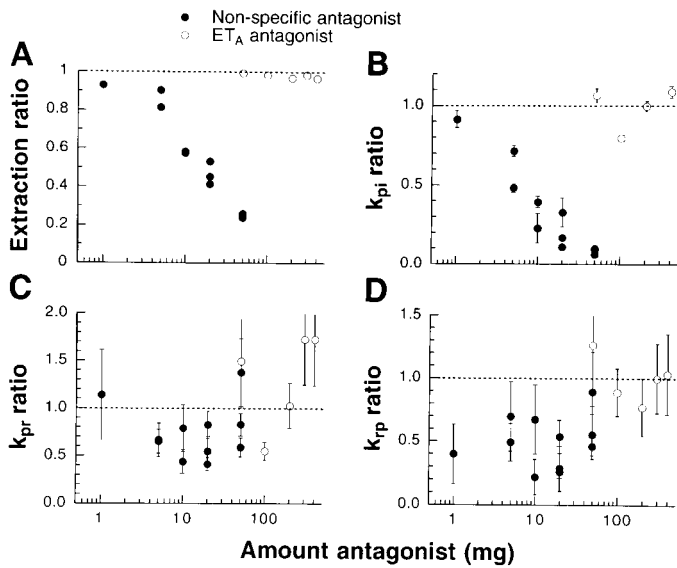


Fig. 4. Variations in ET-1-binding kinetic parameters in dog liver as a function of doses of nonspecific endothelin receptor and specific ET_A receptor antagonists. Parameters are expressed as ratio of value obtained before and after injection of antagonist.

pmol/l with no evident hemodynamic or macroscopic hepatic abnormality during the experiment. Exclusion of this animal from the statistical analysis did not modify the above interpretation, ET-1 levels being 0.39 ± 0.21 pmol/l in the portal vein, 0.24 ± 0.22 pmol/l in hepatic vein, and 0.26 ± 0.22 pmol/l in hepatic artery.

DISCUSSION

ET-1 removal by the liver. We found that ~85% of circulating tracer ¹²⁵I-ET-1 is retained by the liver in a single passage. This represents the highest proportion of removal of ET-1 by an organ reported to date; with the use of a similar technique we previously found that the dog lung removes 33% of circulating ¹²⁵I-ET-1 (4) while the human lung removes 46% (5). The dog myocardium shows a much smaller extraction at 15% (3). If the organ clearance of ¹²⁵I-ET-1 is computed (clearance = organ flow × fractional extraction), the lung remains the major site for ¹²⁵I-ET-1 clearance because it accommodates the whole cardiac output, whereas the hepatic blood flow represents ~25–30% of the total (33).

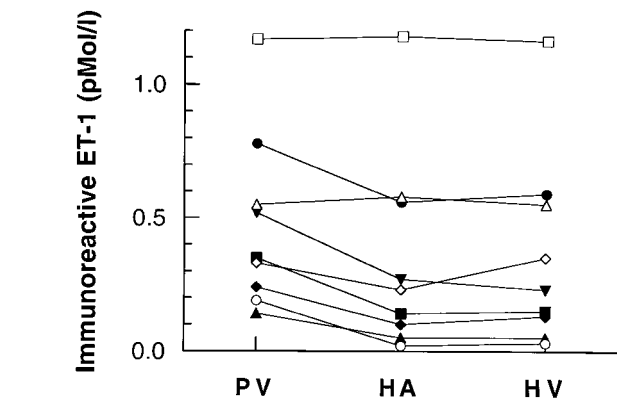


Fig. 6. Individual immunoreactive ET-1 levels in portal vein (PV), hepatic vein (HV), and hepatic artery (HA) from each of 9 experiments without endothelin antagonists

The pulmonary removal of ET-1 is mediated through the endothelial ET_B receptors in dogs (2) and rats (9), with complete inhibition of ET-1 removal after administration of the specific ET_B antagonist BQ-788. The liver and liver-derived cells are rich in both receptor subtypes (23, 24). Hepatic stellate cells show both kinds of receptors, whereas endothelial cells and Kupffer cells only express the ET_B subtype (24). Rat hepatocytes demonstrate high-affinity ET-1 binding sites (11, 31) of both the ET_A and ET_B receptor subtypes (25). Hepatic uptake of ET-1 in rats was found unaffected by the ET_B antagonist BQ-788 (9). The mechanism responsible for ET-1 removal in the liver may consequently be different from that in other organs, with the potential involvement of multiple receptor subtypes.

The present experiments demonstrate that circulating ¹²⁵I-ET-1 is rapidly extracted by the liver. A small portion of ¹²⁵I-ET-1 retained by the liver returns rapidly into the circulation, representing unchanged ET-1 because no metabolites were detected in the hepatic effluent. This is in agreement with observations in rats, in which no appreciable amount of degraded forms of ¹²⁵I-ET-1 have been found in the blood for up to 60 min after intravenous injection (32). The experimental data were quite similar to those obtained with substrates such as galactose or norepinephrine (18, 19). However, the observed binding reversibility stands in sharp contrast to previous observations of virtually irreversible binding of ET-1 to ET_A and ET_B receptors (31, 35).

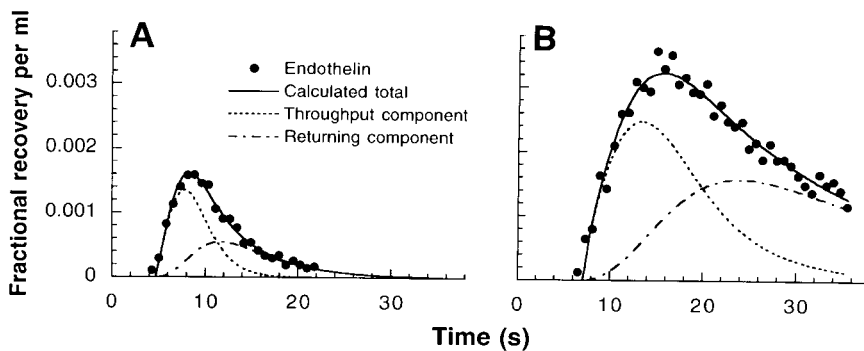


Fig. 5. Theoretical outflow profiles of ET-1, illustrating throughput and returning components in control conditions (A) and after administration of the nonspecific endothelin-receptor antagonist (B).

The hypothesis was therefore put forward that two modes of ET-1 binding exist, one rapid and reversible (occurring on the order of seconds) and one tight and virtually irreversible. In contrast to the case of the liver, reversible retention of ^{125}I -ET-1 was not observed in similar multiple-indicator dilution experiments in the canine myocardium (3) and lung (2). According to this, extraction of ^{125}I -ET-1 as observed in the liver (this study), in the myocardium (3), and in the lung (2) may represent quasi-irreversible binding to surface receptors. With the use of endothelin-receptor antagonists, it was demonstrated that the irreversible binding site responsible for hepatic ET-1 clearance is the ET_B receptor. This result is in accordance with observations in dog lungs, in which ET-1 extraction is exclusively mediated by the endothelial ET_B receptor with no detectable reversible binding by indicator-dilution experiments (2). It is of note that previous hepatic endothelin-receptor binding studies were performed with long incubation times (between 10 min and several hours), with subsequent washing with buffers. Under such conditions, reversible binding with dissociation rate constants as high as those reported here would have been missed. Our results contradict those in rats where hepatic retention of ET-1 was not affected by the ET_B antagonist BQ-788 (9).

The reversible binding site was not dose dependently affected by the nonspecific antagonist, suggesting that this second site is neither an ET_A nor an ET_B receptor. Because no other type of endothelin receptors have been described in mammals, this most likely represents nonspecific binding at the liver surface. The reason why the fitted transfer coefficients for the reversible hepatic binding site tended to be lower, but not dose dependent, with the nonspecific antagonist is unclear. The greater variability and standard errors in the fitted parameters may suggest that this represents experimental variability. Such nonspecific reversible liver binding has previously been postulated for the polypeptide hormone somatostatin, with the use of similar multiple-indicator dilution experiments in the perfused rat liver (29). This is in agreement with the reported absence of somatostatin receptors from the sinusoidal surface of hepatocytes (8).

Multiple indicator dilution experiments with the peptide hormones glucagon and epidermal growth factor have been found to conform to the same barrier-limited model (29). However, an excess of nonlabeled peptide completely suppressed reversible binding as indicated by the abolishment of the returning component in the curves. These peptides are therefore believed to undergo reversible binding to cell-surface receptors, and the one binding site variant of the model was adopted. This is in agreement with reversible binding to cell-surface receptors demonstrated with biophysical measurements with the use of receptors from cancer cell membranes (36) or expressed in single cells (27).

From experiments with human ET_B receptors expressed in single cells (35), a bimolecular rate constant for irreversible ET-1 binding of $\sim 10^{-7}$ M/s can be

derived. With this value and the value for irreversible hepatic ET-1 clearance of $0.17 \text{ ml}\cdot\text{s}^{-1}\cdot\text{g}^{-1}$ from the present work, the receptor density is $\sim 17 \text{ pM/g liver}$.

The majority of labeled ^{125}I -ET-1 is retained in the liver. This is consistent with previous electron-microscopic autoradiographic observations obtained from liver cell cultures showing internalization of labeled ET-1, particularly into hepatic stellate cells (10, 16). A time-dependent reduction of the grain density observed in endothelial and Kupffer cells may be interpreted as a return of unchanged ET-1 after interaction with surface receptors (10). This process, however, is much slower than the return of tracer into the Disse space as assessed with the multiple-indicator dilution technique. The retained ET-1 is most likely metabolized because enzymes capable of ET-1 degradation have been identified both on the cell surface and in the intracellular compartment of liver-derived cells (12).

ET-1 binding to albumin. The hepatic outflow profile of ^{125}I -ET-1 was closely related to that of albumin, suggesting a substantial binding of ET-1 to plasma proteins. This was confirmed by ultrafiltration experiments that demonstrated that 80% of ET-1 was bound to albumin. Others have demonstrated qualitatively important and reversible binding of ET-1 to plasma albumin with the use of gel electrophoresis (34). This binding must, however, show a fast dissociation rate constant because $\sim 85\%$ of circulating ET-1 is extracted within a single transit time through the liver. These observations were therefore incorporated into the modeling analysis by assuming that dissociation of the ET-1-albumin complex had no rate-limiting effect on ET-1 exchanges in the liver and by adjusting the proportion of the Disse space accessible to ET-1 to reflect the partial exclusion of protein-bound ET-1 from this space. This resulted in a good quality of fit.

ET-1 production by the liver. The liver cells have the ability to produce ET-1 that can be used locally in a paracrine fashion but that may also be released into the systemic circulation, where it could act as a circulating hormone. We found a significant statistical difference in the measured ET-1 levels between the portal and the hepatic veins, indicative of a falling ET-1 gradient along the acinar flow path. This difference is, however, of much smaller magnitude than that expected from the important tracer extraction of 85%. This suggests a substantial simultaneous release of ET-1 by the liver into the circulation in excess of what is predicted from returning tracer. ET-1 may either be newly synthesized in the liver or stored for time periods largely exceeding the time of sample collection. We cannot, however, quantify this release because we have not measured hepatic artery and portal blood flow separately in our preparation. Our results nevertheless firmly establish for the first time, in vivo, that the liver not only has the ability to remove but also to release ET-1 into circulation. This view is confirmed by the recent finding of ET-1 mRNA in the rat liver, which was most abundant in endothelial cells, and increased ninefold 3 h after a bolus infusion of endotoxin into a mesenteric vein (6).

Our results demonstrate both substantial clearance and production of ET-1 by the intact liver. Hepatic ET-1 clearance is mediated by the ET_B receptor, with the presence of reversible, nonspecific ET-1 binding at the liver surface. Whether alterations of hepatic ET-1 metabolism in chronic liver disease may contribute to the observed increase in circulating ET-1 levels through a reduction in clearance, an increase in production, or a combination of both will require further studies.

We thank Eva Ibrahim, Bruce Ritchie, and Kay Lumsden for expert technical assistance as well as Diane Campeau for help in typing this manuscript.

This work was supported by the Medical Research Council of Canada, the Fonds de la recherche en santé du Québec, the Quebec Heart and Stroke Foundation, the Fonds de recherche de l'Institut de Cardiologie de Montréal, and the Fast Foundation.

Address for reprint requests and other correspondence: J. Dupuis, Research Center, Montreal Heart Institute, Montreal, PQ, Canada H1T 1C8.

Received 11 February 1998; accepted in final form 10 June 1999.

REFERENCES

1. **Änggård, E., S. Galton, G. Rae, R. Thomas, L. McLoughlin, G. de Nucci, and J. R. Vane.** The fate of radioiodinated endothelin-1 and endothelin-3 in the rat. *J. Cardiovasc. Pharmacol.* 13, *Suppl.* 5: S36–S44, 1989.
2. **Dupuis, J., C. A. Goresky, and A. Fournier.** Pulmonary clearance of circulating endothelin-1 in dogs in vivo: exclusive role of ET_B receptors. *J. Appl. Physiol.* 81: 1510–1515, 1996.
3. **Dupuis, J., C. A. Goresky, C. P. Rose, D. J. Stewart, and P. Cernacek.** Endothelin-1 myocardial clearance and production and effect on capillary permeability in vivo. (Abstract). *J. Am. Coll. Cardiol.* 27, *Suppl.* A: 322A, 1996.
4. **Dupuis, J., C. A. Goresky, and D. J. Stewart.** Pulmonary removal and production of endothelin in the anesthetized dog. *J. Appl. Physiol.* 76: 694–700, 1994.
5. **Dupuis, J., D. J. Stewart, P. Cernacek, and G. Gosselin.** Human pulmonary circulation is an important site for both clearance and production of endothelin-1. *Circulation* 94: 1578–1584, 1996.
6. **Eakes, A. T., K. M. Howard, J. E. Miller, and M. S. Olson.** Endothelin-1 production by hepatic endothelial cells: characterization and augmentation by endotoxin exposure. *Am. J. Physiol.* 272 (*Gastrointest. Liver Physiol.* 35): G605–G611, 1997.
7. **Elshourbagy, N. A., D. R. Korman, H. L. Wu, D. R. Sylvester, J. A. Lee, P. Nuthalaganti, D. J. Bergsma, C. S. Kumar, and P. Nambi.** Molecular characterization and regulation of the human endothelin receptors. *J. Biol. Chem.* 268: 3873–3879, 1993.
8. **Fricker, G., V. Dubost, D. Schwab, C. Bruns, and C. Thiele.** Heterogeneity in hepatic transport of somatostatin analog octapeptides. *Hepatology* 20: 191–200, 1994.
9. **Fukuroda, T., T. Fujikawa, S. Ozaki, K. Ishikawa, M. Yano, and M. Nishikibe.** Clearance of circulating endothelin-1 by ET_B receptors in rats. *Biochem. Biophys. Res. Commun.* 199: 1461–1465, 1994.
10. **Furuya, S., S. Naruse, T. Nakayama, and K. Nokihara.** Binding of ¹²⁵I-endothelin-1 to fat-storing cells in rat liver revealed by electron microscopic radioautography. *Anat. Embryol. (Berl.)* 185: 97–100, 1992.
11. **Gandhi, C. R., R. H. Behal, S. A. Harvey, T. A. Nouchi, and M. S. Olson.** Hepatic effects of endothelin. Receptor characterization and endothelin-induced signal transduction in hepatocytes. *Biochem. J.* 287: 897–904, 1992.
12. **Gandhi, C. R., S. A. Harvey, and M. S. Olson.** Hepatic effects of endothelin: metabolism of [¹²⁵I]endothelin-1 by liver-derived cells. *Arch. Biochem. Biophys.* 305: 38–46, 1993.
13. **Gandhi, C. R., L. A. Sproat, and V. M. Subbotin.** Increased hepatic endothelin-1 levels and endothelin receptor density in cirrhotic rats. *Life Sci.* 58: 55–62, 1996.
14. **Gandhi, C. R., K. Stephenson, and M. S. Olson.** A comparative study of endothelin- and platelet-activating-factor-mediated signal transduction and prostaglandin synthesis in rat Kupffer cells. *Biochem. J.* 281: 485–492, 1992.
15. **Gandhi, C. R., K. Stephenson, and M. S. Olson.** Endothelin, a potent peptide agonist in the liver. *J. Biol. Chem.* 265: 17432–17435, 1990.
16. **Gondo, K., T. Ueno, M. Sakamoto, S. Sakisaka, M. Sata, and K. Tanikawa.** The endothelin-1 binding site in rat liver tissue: light- and electron-microscopic autoradiographic studies. *Gastroenterology* 104: 1745–1749, 1993.
17. **Goresky, C. A.** A linear method for determining liver sinusoidal and extravascular volumes. *Am. J. Physiol.* 204: 626–640, 1963.
18. **Goresky, C. A., G. G. Bach, D. Cousineau, A. J. Schwab, C. Rose, S. Lee, and S. Goresky.** Handling of tracer norepinephrine by the dog liver. *Am. J. Physiol.* 256 (*Gastrointest. Liver Physiol.* 19): G107–G123, 1989.
19. **Goresky, C. A., G. C. Bach, and B. E. Nadeau.** On the uptake of materials by the intact liver. The transport and net removal of galactose. *J. Clin. Invest.* 52: 991–1009, 1973.
20. **Goresky, C. A., G. G. Bach, and A. J. Schwab.** Distributed-in-space product formation in vivo: enzymic kinetics. *Am. J. Physiol.* 264 (*Heart Circ. Physiol.* 33): H2029–H2050, 1993.
21. **Goresky, C. A., and M. Silverman.** Effect of the correction of catheter distortion on calculated liver sinusoidal volumes. *Am. J. Physiol.* 207: 883–892, 1964.
22. **Goresky, C. A., A. Simard, and A. J. Schwab.** Increased hepatocyte permeability surface area product for ⁸⁶Rb with increase in blood flow. *Circ. Res.* 80: 645–654, 1997.
23. **Hochoer, B., R. Zart, F. Diekmann, T. Slowinski, C. Thone-Reineke, J. Lutz, and C. Bauer.** Protective effects of the mixed endothelin receptor antagonist bosentan in rats with CCl₄-induced liver injury. *J. Cardiovasc. Pharmacol.* 26, *Suppl.* 3: S130–S131, 1995.
24. **Housset, C., D. C. Rockey, and D. M. Bissell.** Endothelin receptors in rat liver: lipocytes as a contractile target for endothelin 1. *Proc. Natl. Acad. Sci. USA* 90: 9266–9270, 1993.
25. **Jouneaux, C., A. Mallat, C. Serradeil-Le Gal, P. Goldsmith, J. Hanoune, and S. Lotersztajn.** Coupling of endothelin B receptors to the calcium pump and phospholipase C via G_s and G_q in rat liver. *J. Biol. Chem.* 269: 1845–1851, 1994.
26. **Moore, K., J. Wendon, M. Frazer, J. Karani, R. Williams, and K. Badr.** Plasma endothelin immunoreactivity in liver disease and the hepatorenal syndrome. *N. Engl. J. Med.* 327: 1774–1778, 1992.
27. **Rousseau, D. L., Jr., J. V. Staros, and J. M. Beechem.** The interaction of epidermal growth factor with its receptor in A431 cell membranes: a stopped-flow fluorescence anisotropy study. *Biochemistry* 34: 14508–14518, 1995.
28. **Sakurai, T., M. Yanagisawa, Y. Takuwa, H. Miyazaki, S. Kimura, K. Goto, and T. Masaki.** Cloning of a cDNA encoding a non-isopeptide-selective subtype of the endothelin receptor. *Nature* 348: 732–735, 1990.
29. **Sato, H., Y. Sugiyama, Y. Sawada, T. Iga, S. Sakamoto, T. Fuwa, and M. Hanano.** Dynamic determination of kinetic parameters for the interaction between polypeptide hormones and cell-surface receptors in the perfused rat liver by the multiple-indicator dilution method. *Proc. Natl. Acad. Sci. USA* 85: 8355–8359, 1988.
30. **Sebille, B.** Methods of drug protein binding determinations. *Fundam. Clin. Pharmacol.* 4, *Suppl.* 2: 151s–161s, 1990.
31. **Serradeil-Le Gal, C., C. Jouneaux, A. Sanchez-Bueno, D. Raufaste, B. Roche, A. M. Preaux, J. P. Maffrand, P. H. Cobbold, J. Hanoune, and S. Lotersztajn.** Endothelin action in rat liver. Receptors, free Ca²⁺ oscillations, and activation of glycogenolysis. *J. Clin. Invest.* 87: 133–138, 1991.
32. **Shiba, R., M. Yanagisawa, T. Miyauchi, Y. Ishii, S. Kimura, Y. Uchiyama, T. Masaki, and K. Goto.** Elimination of intravenously injected endothelin-1 from the circulation of the rat. *J. Cardiovasc. Pharmacol.* 13, *Suppl.* 5: S98–S101, 1989.
33. **Skerjanec, A., D. W. O'Brien, and T. K. Tam.** Hepatic blood flow measurements and indocyanine green kinetics in a chronic dog model. *Pharm. Res.* 11: 1511–1515, 1994.

34. **Sorensen, S. S.** Radio-immunoassay of endothelin in human plasma. *Scand. J. Clin. Lab. Invest.* 51: 615–623, 1991.
35. **Takasuka, T., M. Adachi, C. Miyamoto, Y. Furuichi, and T. Watanabe.** Characterization of endothelin receptors ET_A and ET_B expressed in COS cells. *J. Biochem. (Tokyo)* 112: 396–400, 1992.
36. **Tota, M. R., L. Xu, A. Sirotina, C. D. Strader, and M. P. Graziano.** Interaction of [fluorescein-Trp25]glucagon with the human glucagon receptor expressed in *Drosophila* Schneider 2 cells. *J. Biol. Chem.* 270: 26466–26472, 1995.
37. **Xu, X., A. J. Schwab, F. Barker, C. A. Goresky, and K. S. Pang.** Salicylamide sulfate cell entry in perfused rat liver: a multiple-indicator dilution study. *Hepatology* 19: 229–244, 1994.
38. **Zhang, J. X., W. Pegoli, Jr., and M. G. Clemens.** Endothelin-1 induces direct constriction of hepatic sinusoids. *Am. J. Physiol.* 266 (*Gastrointest. Liver Physiol.* 29): G624–G632, 1994.

